Egyptian Journal of Aquatic Biology & Fisheries
Zoology Department, Faculty of Science,
Ain Shams University, Cairo, Egypt.
ISSN 1110 – 6131
Vol. 26(4): 289 – 309 (2022)
www.ejabf.journals.ekb.eg

Distribution of Natural radionuclides and its Associated Hazards in the Valleys Coastline of the Red Sea, Egypt

Amany G. Madkour [1]*, Mohamed E.A. El-Metwally [1], Hesham M.H. Zakaly [2], Lamiaa I. Mohamedein [1], Shams A.M. Issa [2], Ahmed R. Elgendy [1]

1. National Institute of Oceanography and Fisheries (NIOF), Egypt.
2. Physics Department, Faculty of Science, Al-Azhar University, 71524, Assuit, Egypt.

***Corresponding Author:** dramanymadkour@yahoo.com

ARTICLE INFO

Article History:
Received: May 25, 2022
Accepted: July 2, 2022
Online: July 19, 2022

Keywords:
Radiation hazards,
Radionuclides,
Dose rate,
Cancer risk,
The Red Sea valleys

ABSTRACT

The current study introduced the activity levels of ^{238}U, ^{232}Th, and ^{40}K as well as their radiological hazard indices for some valleys along the Gulf of Suez and the Red Sea. Activity levels of ^{238}U, ^{232}Th, and ^{40}K were performed by a ϒ-ray spectrometer at the Nuclear and Radiological Regulation Authority (CLERMIT), Egypt, using a NaTl detector (3x3 inch). "Genie-2000" program has been used to analyze the gamma-ray spectrum. The mean activity levels of ^{238}U ranged from 6.10Bq/kg to 157.68Bq/kg, ^{232}Th fluctuated between 4.38Bq/kg and 29.92Bq/kg, and ^{40}K changed from 44.80Bq/kg to 497.18Bq/kg. The calculated absorbed and effective dose rate values in the downstream and the tidal flat of Hamrawin valley reached 76.41 and 88.39nGyh^{-1}; the annual effective dose-effect was 93.71, and 108.40Sv Gy^{-1}; the radium equivalent activity level index values were 163.59 and 190.01Bq kg, and the external hazard index reached (0.44 and 0.51). The representative level index values reached 1.16 and 1.30, and the excess lifetime cancer risk reached 0.27×10^{-3} in the valley downstream and 0.31×10^{-3} in the tidal flat zone, respectively. The radiological risk parameters values of (D), (AEDE), (Iγr), and (ELCR) at the Hamrawin valley are not safe, exposing health risks to the population, since they are higher than the permissible levels.

INTRODUCTION

Radioactivity from naturally occurring radioactive materials (NORMs) is ubiquitous in the terrestrial environment and exists in various geological formations, viz. soils, rocks, sediment, air, and construction materials **(Ramasamy *et al.*, 2013; Abbasi *et al.*, 2022)**. However, the distribution of NORMs in the terrestrial and coastal sediments relies on both the distribution of rocks and the procedures through which they are concentrated. **Noureddine *et al*. (1998)** and **Mahur *et al*. (2010)** reported that, the major source of natural radionuclides in the aquatic environment results from the weathering and recycling of terrestrial minerals and rocks that give rise to ^{40}K, ^{232}Th and ^{238}U in marine sediments **(Zakaly *et al*., 2021)**.

Human and other organisms alive are inevitably exposed to some amount of ionizing radiations from the NORMs ^{238}U, ^{232}Th, and ^{40}K in the soil, sediments and streams, lakes, and other environmental samples **(El Samad *et al*., 2013; Yücel *et al*., 2020)**. It was estimated that about 87% of the radiation doses received by humans are from natural sources, produced by radioactive isotopes of ^{238}U and ^{232}Th in addition to their progeny and ^{40}K **(UNSCEAR, 2008; Shetty & Narayana, 2010)**. The effects of radiation on humans and biota vary according to the radiation type (α or β or γ), the time of exposure, the dose, and the exposure route (external, inhalation, and ingestion) **(ATSDR, 1988; INRS, 2012; El Zrelli *et al*., 2019)**. A long exposure period leads to a greater risk of cancer (including lung, breast, and thyroid glands) that usually appear after decades of exposure **(UNSCEAR, 2000)**. Therefore, it is important to estimate the potential hazards of natural radiation for the human health and to protect the natural environment **(Ramasamy *et al*., 2013)**.

Previous studies showed that some areas around the world (France, Australia and China) have elevated background radiation levels as a result of the occurrence of elevated NORMs in soil, rocks and sediments. Phosphate rocks and ores around the world contain significantly high levels of ^{238}U, ^{232}Th series, and ^{40}K. Therefore, the mining and the processing of phosphates and subsequent spread of phosphate-containing dust in the environment are considered a major source of contamination with naturally radioactive materials **(Shetty & Narayana, 2010; El Zrelli *et al*., 2019)**.

Egypt's phosphate ore deposits are a part of the Mediterranean Phosphate Province, which is located in the Mediterranean Sea, where the Red Sea Mountains and the coastal areas are considered the main center for mining, processing, and shipping of phosphates in Egypt **(El Mamoney & Khater, 2004)**. In addition, high radiation levels are connected to igneous rocks such as granite, which is widely distributed in the eastern desert of Egypt **(El-Gamal *et al*., 2018)**. Considerable amounts of these phosphate ores and other materials reach the marine environment throughout shipping operations and with flash floods via several valleys along the Gulf of Suez and the Red Sea **(Salah el Din & Vesterbacka, 2012)**. Previous studies **(Seddeek *et al*., 2005; Dar & Saman, 2012; El-Taher *et al*., 2018b)** have reported high levels of natural radionuclides in marine sediments, associated with phosphate mining and shipping. However, there is still lacking information regarding the natural radiation hazards of the valleys as well as the hazards to human health and the marine environment.

The present work aimed to assess the natural activity levels of ^{238}U, ^{232}Th, and ^{40}K in sediment samples collected from some valleys downstream and the tidal flat zones in front of the valleys outfalling along the Gulf of Suez and the Red Sea. In addition, the study targeted the assessment of the radiological hazards associated with these radionuclides in the investigated areas. To achieve the objectives of this work, the research was conducted in six valleys along the Gulf of Suez and the Red Sea, Egypt during 2018.

MATERIALS AND METHODS

1. *Study Areas*

Al Galala Valley is located at the northern tip of Suez Gulf at the Industrial Area of Northern Suez Gulf, Soumed Terminal Station and Harbor, Dubai Harbors Company, and in an area with many industrial and tourist activities. The valley is annually active and has a heavy load of flash floods from the neighbour mountains that threaten the locality. Two main drains were observed for this valley; one of them extended northern of Soumed Terminal Station, and the other was found to the South of this station and extended to the Gulf. The southern drain of the valley is active most of the year and is covered with dense vegetation.

Araba Valley has a very wide downstream which drains directly in Suez Gulf northern of Zafarana Village and has an annually heavy load of flashflood. Most of the downstream are covered with dense vegetation due to the presence of freshwater all over the year. The area around the downstream is exploited in tourist and recreational activities.

Umm Hawytat Valley is situated about 15km south of Safaga City, and its downstream drains directly in the Red Sea. This valley extends from the Red Sea Mountains with many distributaries and has temporarily flashfloods, approximately every five years. The upstream area of the valley is occupied by small Umm Hawytat occupation town. About 5,000 people are working in mining, and governmental services many mines are found in the locality. The downstream is very wide, followed by an extended tidal flat enriched with the ethnic communities.

Hamrawin territory involves the largest phosphate mines, a manufacturing plant for milling, and a port on the Red Sea coast. Hamrawin phosphate port is on a small embayment to the south **(Dar, 2005)** of Hamrawin valley, which the phosphate comes from. Two main downstream paths for V. Hamrawin, south and northern the occupation area and the ore grinding factory.

Ambagy Valley is a path through the southern part of Qusier City. The downstream of the valley is described by the occupation of large population with few tourist activities and temporary flashfloods (each 10 to 20 years).

Abu Dabab Valley formed a tiny fault in the submersible coastal terrace of the Red Sea. The tidal flat and marine area of the valley downstream are described by varied and prolific coral communities, which are deeply exploited as diving places that expand the anthropogenic stress in the marine constituents of the locality **(Fig. 1)**.

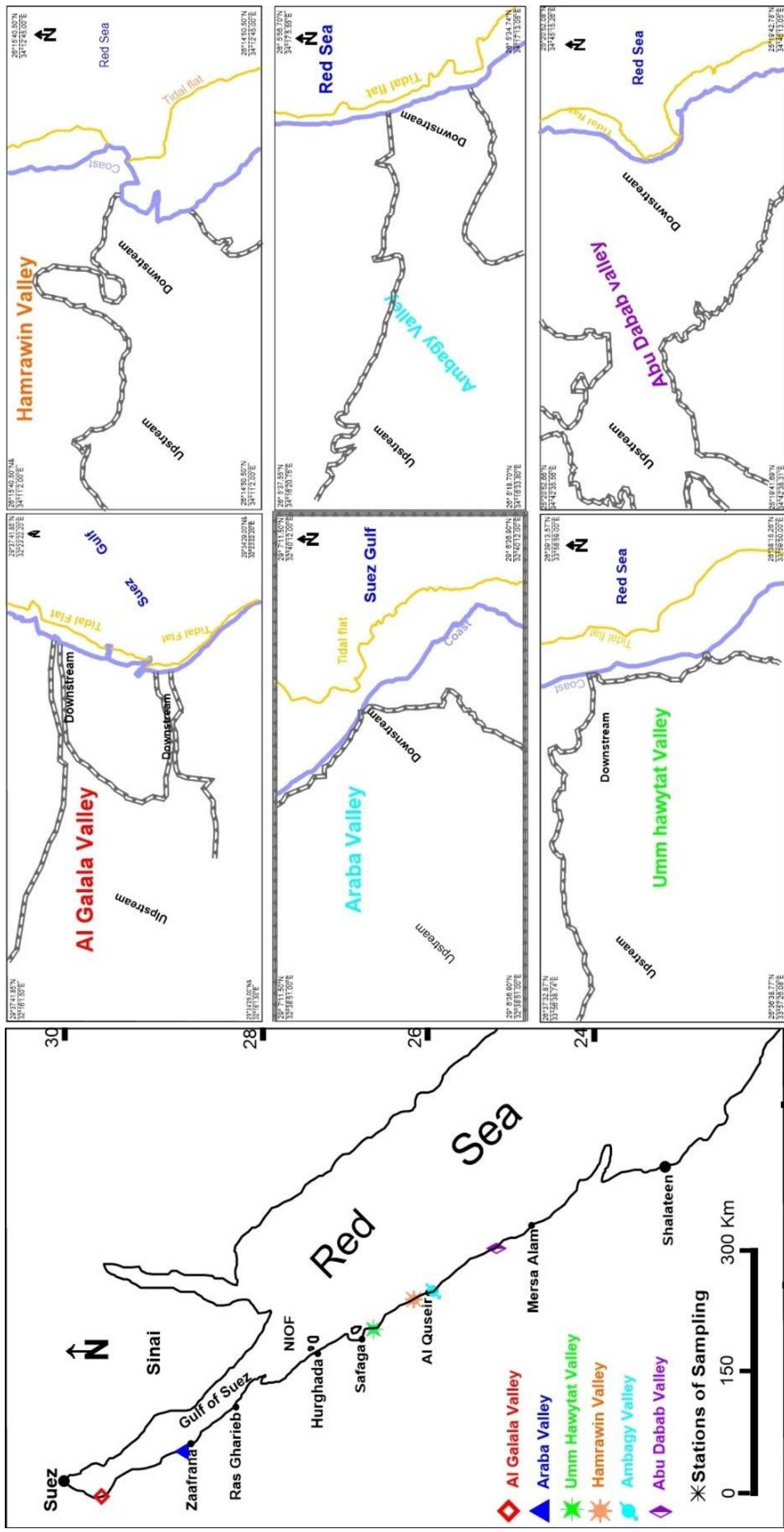

Fig. 1. Location map illustrating the studied Valleys.

2. Fieldwork:

Throughout five field trips along the Gulf of Suez and the Red Sea covering a distance of 750km during 2018, 57 sediment specimens have been handly collected, and snorkeling from the selected valleys represents the downstream and the flat tidal area of each valley.

3. Analysis:

In the Lab., the collected specimens have been air-dried, about 100 g of the sample intended for the grain size analyses each one phi (Ø) interval according to **(Boggs, 2009)**. The obtained fractions were; gravel $Ø_{-1}$ (>2.00mm), very coarse sand $Ø_0$ (2.00:1.00mm), coarse sand $Ø_1$ (1.00:0.50mm), medium sand $Ø_2$ (0.50-0.25mm), fine sand $Ø_3$ (0.25:0.125mm), very fine sand $Ø_4$ (0.126:0.063mm) and mud fraction $Ø_5$ (<0.063mm). The different sediment categories were grouped into three groups; Coarse Sediment Group CSG ($Ø_{-1}$+$Ø_0$), Medium Sediment Group MSG ($Ø_1$+$Ø_2$), and Fine Sediment Group FSG ($Ø_3$+$Ø_4$+$Ø_5$). About 0.250 kg homogenized and air-dried specimen has been dried in furnace at 110^{o}C to take off moisture. The specimens have been powdered utilizing mortar to < 80 mesh (177µm) then to occur secular equilibrium, All specimens have been saved in closed container for twenty-eight days where the rate of disintegration of the progeny be egalitarian to that of the parent (Ra and Th), and the progeny will exist in the specimen **(Ravichandran *et al*., 2019) (ASTM 1983, 1986)**.

The activity levels of ^{238}U, ^{232}Th, and ^{40}K were performed by a ϒ-ray spectrometer at the Nuclear and Radiological Regulation Authority (CLERMIT), Egypt, using a NaTl detector (3x 3 inch). "Genie-2000" program has been used to analysis the gamma-ray spectrum. The ^{232}Th level was measured from the average levels of ^{212}Pb and ^{228}Ac with 238.6 and 911.1 keV, respectively. The ^{238}U was measured using ^{214}Pb and ^{214}Bi at gamma lines 351.9, 609.3, and 1764.5 keV, respectively. In contrast, the gamma line for ^{40}K is 1460.6 keV. The minimum detectable activities (MDA) were 25.2, 6.5, and 5.7 Bq/kg for ^{40}K, ^{238}U, and ^{232}Th as described by **(Dar *et al*., 2015; Zakaly *et al*., 2019)**, respectively.

4. Radiological Hazard Indices Calculations:

4.1. Absorbed and effective dose rate (D):

The absorbed dose rate (D) in the air at 1m above the ground surface for the naturally occurring radioisotopes (^{238}U, ^{232}Th, and ^{40}K) was calculated according to **(UNSCEAR, 2000)**. The conversion factors were utilized to evaluate the D values in the air are 0.462, 0.604, and 0.0417 Bq/kg for ^{238}U, ^{232}Th, and ^{40}K, respectively. Therefore D values have been evaluated as follows **(UNSCEAR, 2000)**:

$$\boldsymbol{D}\ (\mathrm{nGy\ h^{-1}}) = 0.462C_U+0.604C_{Th}+0.0417C_K$$

Where C_U, C_{Th}, and C_k are the activity levels of ^{238}U, ^{232}Th, and ^{40}K in Bq/kg, respectively.

4.2. The annual effective dose effect (AEDE):

(AEDE) was estimated in (μSv/y) according to the following formula **(UNSCEAR, 2000)**:

AEDE **(Al-Trabulsy *et al*., 2011)** = (D) (24 h) (365.25 day) (0.2, occupancy factor) (7×10^{-4}, conversion coefficient)

4.3. Radium equivalent (Raeq):

(Ra_{eq}) describe the gamma emitted from uranium, thorium, and potassium mixtures in specimens from various sites. Ra_{eq} was computed using **(Beretka and Mathew, 1985)**:

$Ra_{eq} = C_U + 1.43C_{Th} + 0.077C_K$

This equation is based on the assumption that 10, 7, and 130 Bq/kg of ^{238}U, ^{232}Th, and ^{40}K produce the similar D.

4.4. External hazard index (Hex):

H_{ex} is the external exposure related to gamma irradiation from the natural radionuclides, in the selected locations. It was computed using the equation of **(Janković *et al*., 2008):**

$H_{ex} = (C_U/370 + C_{Th}/259 + C_K/4810) \le 1$

To hold the radiation risk insignificant, the H_{ex} should be less than unity.

4.5. Representative level index (Iγr):

(Iγr) is manipulated using the equation **(Awad *et al*., 2021)**:

$I\gamma r = (C_U/150 + C_{Th}/100 + C_K/1500) < 1$

As the H_{ex}, The value of $I_{\gamma r}$ must be <1

4.6. The excessive lifetime cancer risk (ELCR):

(ELCR) gives eventuality Prevalence of the risk of cancer disease over a long period at a given exposure level. It was calculated using AEDE values as the following:

ELCR = (*AEDE)* (DL, the average length of one's life) (RF, 0.05 Sv^{-1})

Where RF is the fatal cancer risk per Sv **(Taskin *et al*., 2009)**.

RESULTS

1. Granulometric analysis:

The majority of natural radionuclides in the sediments are attached by the fine fractions with diameters < 2×10^{-3} cm; more significant fractions contain only traces of these radionuclides **(Nasr *et al*., 2006)**. ^{238}U has the tendency to accumulate in the finest sediments much more than the medium and coarse sediments **(Noureddine *et al*., 1998)**. These radionuclides are absorbed onto SPM in the water column and then settle out in the seabed sediment **(Bell *et al*., 1997)**. In the present study, the fine sediment fraction $Ø_4$ and the fine sediment group FSG are prevailing the most of samples at the downstream areas of the different valleys except V. Umm Hawytat, where the FSG group is almost equal to MSG group (37.6 and 37.25% respectively); meanwhile, MSG group recorded the highest percentage at V. Ambagy (40.25%). The highest percentage of FSG group was recorded at V. Hamrawin downstream (79.39%) due to the dust and smoothers from pulverizing and milling the raw boulders and large stones at Phosphate Grinding Factory. The raw materials contain a mixture of all grain sizes. On most days, the transferred raw materials were exposed to intensive winds throughout the shipping process. Then, the precisest particles of raw materials in the air fall in the marine area and the adjoining zone. On days when the wind is blowing in the opposite direction, the amount of volatilized materials doubled to more than 4 or 5 folders due to the produced eddy winds that increase the fell raw materials to the marine zone around the port **(Dar, 2005)**. In the tidal flat zones as in the downstream valleys, FSG and Ø4 recorded the highest percentages except for V. Umm Hawytat, whereas MSG showed the highest percentage (49.61%). At the tidal flat of V. Al Galala, FSG and MSG groups recorded nearly equal percentages (48.12 and 46.4%). The tidal flat of V. Hamrawin recorded a significantly high FSG group (82.08 %), this is due to thrown terrestrial runoff from the phosphate shipment operations as well as the flash floods **(El-mamoney & Rifaat, 2001)**, while the lowest percentage recorded at Umm Hawytat tidal flat (36.54%) **(Fig. 2)**.

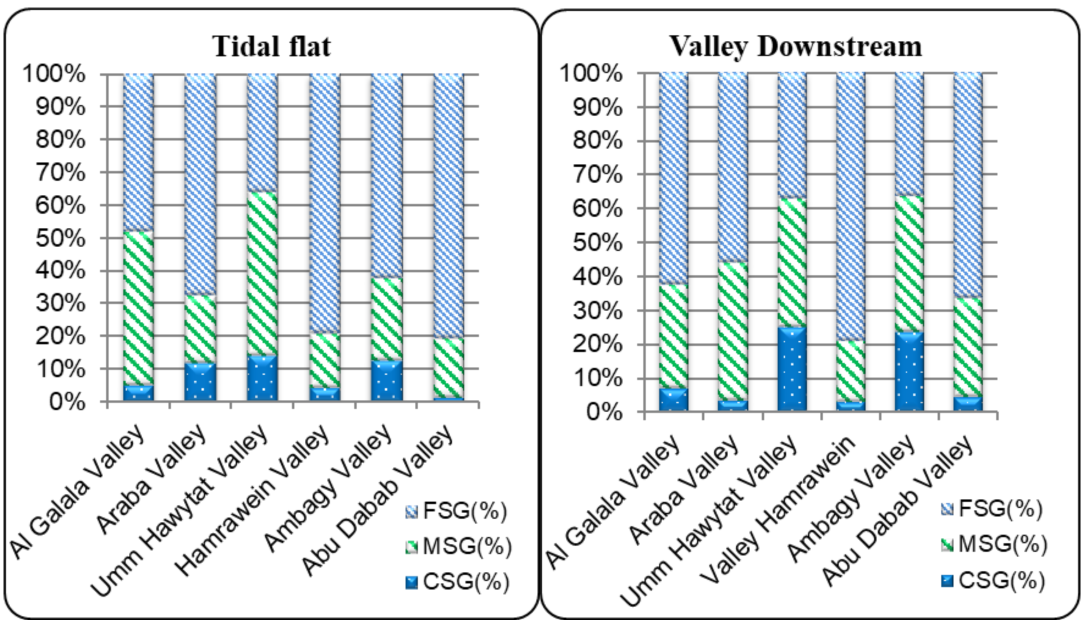

Fig. 2. The Distributions pattern of different sediment groups percentage (CSG, MSG, and FSG %) of areas of the study valleys during 2018.

As shown in **(Table 1)** in the downstream zones, ^{238}U showed a strong positive correlation with FSG percentage at V. Ambagy downstream (r= 0.80), ^{232}Th recorded fair to strong positive correlations with FSG percentages at V. Ambagy and V. Abu Dabab (r= 0.69 & 0.59) and fair negative at V. Al Galala (r=-0.63). Meanwhile, ^{40}K showed a fair, positive correlation with FSG at V. Ambagy (r=0.53) and fair to good negative correlations With FSG at V. Al Galala and V. Umm Hawytat (r=-0.64 and -0.75). In the tidal flat zones of the studied valleys, ^{238}U, ^{232}Th, and ^{40}K showed excellent positive correlations with FSG percentage (r=1.00) at V. Umm Hawytat, ^{238}U recorded strong to excellent negative relationships with FSG at V. Hamrawin, V. Ambagy, and V. Abu Dabab (r= -0.79, -0.75 and -1.00), ^{232}Th recorded strong positive at V. Al Galala (r=0.75) and excellent positive at V. Abu Dabab (r=1.00). ^{40}K Showed a strong positive with FSG at V. Araba and V. Hamrawin (r=0.85 and 0.80) and excellent negative at V. Abu Dabab (r=-1.00). The positive correlations mean that the FSG is the probable source of the recorded activities. Meanwhile, the negative correlations indicated that CSG and MSG are the probable sources. The positive correlations between FSG and ^{232}Th mean that these valleys continuously receive fresh sediments in both downstream and tidal flats; this investigation was supported by the field observations like in V. Al Galala, V. Araba, and V. Hamrawin.

Table 1. Correlation Coefficients illustrate the relation between the FSG% and the radionuclides (^{238}U, ^{232}Th, and ^{40}K) in the sediment samples at the studies valleys during 2018.

Sites	Downstream			Tidal flat		
	^{238}U	^{232}Th	^{40}K	^{238}U	^{232}Th	^{40}K
V. Al Galala	0.16	-0.63	-0.64	-0.45	0.75	0.39
V. Araba	0.40	-0.39	-0.07	0.38	-0.39	0.85
V. Umm Hawytat	-025	-0.23	-0.75	1.00	1.00	1.00
V. Hamrawin	0.11	0.38	0.01	-0.79	0.47	0.80
V. Ambagy	0.80	0.69	0.53	-0.75	-0.13	-0.17
V. Abu Dabab	0.36	0.59	0.40	-1.00	1.00	-1.00

2. Radioactivity and radiation hazards:

2.1. Activity levels of ^{238}U, ^{232}Th and ^{40}K:

The activity levels of the natural radionuclides (^{238}U, ^{232}Th, and ^{40}K) in sediment samples of the studied valleys along the Gulf of Suez and the Red Sea are reported in **(Tables 2, 3)**. In the downstream zones, V. Hamrawin recorded the highest ^{238}U activity (93.20Bq/kg) meanwhile; V. Ambagy recorded the lowest activity (20.30Bq/kg). The increased activities of ^{238}U at V. Hamrawin were attributed definitely to the phosphate ores in the locality, dust, and smoothers from the grinding factory, and shipment operations at the Harbor in addition to the temporary flash floods. The recorded average activity of ^{238}U at the study valleys was found higher than those recorded in El-Salam Canal **(Ramadan *et al*., 2018)**, Red Sea **(Salama *et al*., 2015)**, Burullus and Marriot lakes **(Dar & El Saharty, 2013)**, Ras El Behar and Hamrawin, Red Sea **(Dar & Saman, 2012)**; Red Sea sediments **(El Saharty & Dar, 2010)**, Brullus Lake **(El-Reefy *et al*., 2010)**, and Idku Lake **(Fahmi *et al*., 2010)**. **(Table 4)**. ^{232}Th showed the high activity at V. Araba (29.92Bq/kg) followed by V. Hamrawin downstream (27.98Bq/kg) and V. Al

Galala (27.36Bq/kg) and the lowest activities (at 14.53Bq/kg) was recorded at V. Abu Dabab downstream. The recorded high activities of ^{232}Th in the downstream of V. Araba and V. Al Galala were attributed to the fresh sources of sediments from the continuous heavy loads flash floods, meanwhile, at V. Hamrawin downstream could be due to the artificial sources from phosphate ores, dust, and smoothers from shipment operations. The average activities of ^{232}Th recorded at the study valleys were found higher than the recorded activity in Hamrawin **(Salah el Din & Vesterbacka, 2012)**, Safaga and Hurghada sands **(El-Arabi, 2005)**; Quseir harbor, Abu tartour harbor, Touristic harbor and Hurghada harbors **(El-Taher *et al*., 2018a)**, El Salam Canal **(Ramadan *et al*., 2018)**, Red Sea **(Salama *et al*., 2015)**, Burullus and Mariout lakes **(Dar & El Saharty, 2013)**, Ras El Behar and Hamrawin, Red Sea **(Dar & Saman, 2012)**, Red Sea sediments **(El Saharty & Dar, 2010)**, Brullus Lake **(El-Reefy *et al*., 2010)**, Safaga and Hurghada Red Sea **(El-Arabi, 2005)** and Nasser Lake **(Khater *et al*., 2005)**. However, it was much lower than those recorded at Shore sediment **(El Mamoney & Khater, 2004)** and Zaranik, North Sinai **(Seddeek *et al*., 2005)** and Suez Canal **(El-Tahawy *et al*., 1994)**. **(Table 4)**.

In all studied valleys, the highest activity of ^{40}K was observed at V. Umm Hawytat downstream (497.18Bq/kg) followed by V. Araba downstream (426.45Bq/kg) and the lowest one (296.23Bq/kg) was at V. Ambagy. The high activities of ^{40}K at both V. Umm Hawytat and V. Araba indicated that the essential sources of terrestrial runoff are from granitic sources at the Red Sea Mountains which are enriched by potash feldspars. **(Jacobi, 1988; Al-Trabulsy *et al*., 2011)** The conclusion was reached that the phosphate industry has been identified as a significant source of natural radionuclides, which can be traced back to industrial operations involving phosphate ores.

^{40}K recorded activities at the study valleys were found near to those recorded in Quseir harbor, Abu Tartor Harbor, and Hurghada Harbor **(El-Taher *et al*., 2018a)** and lower those recorded in Touristic Harbor **(El-Taher *et al*., 2018a)**, Mariout lake **(Dar & El Saharty, 2013)**, Red Sea sediments **(El Saharty & Dar, 2010)** and Safaga and Hurghada sand **(El-Arabi, 2005)**. **(Table 4)**.

On the other hand, the recorded activities were greater those reported in Hamrawin **(Salah el Din & Vesterbacka, 2012)**, Shore sediment **(El Mamoney & Khater, 2004)**, Zaranik, North Sinai **(Seddeek *et al*., 2005)**, El Salam canal **(Ramadan *et al*., 2018)**, Burullus Lake **(Dar & El Saharty, 2013)**, Ras El Behar and Hamrawin, Red Sea **(Dar & Saman, 2012)**, Idku Lake **(Fahmi *et al*., 2010)**, Nasser Lake **(Khater *et al*., 2005)** and Red Sea **(Salama *et al*., 2015)**. **(Table 4)**.

In the tidal flat zones, the significantly high activity of ^{238}U was also recorded at V. Hamrawin tidal flat (157.68Bq/kg) whereas huge quantities of phosphate rows were fallen in the marine area inside and around the navigation basin during shipment operations whereas the significant low activity (4.40Bq/kg) was observed at Umm Hawytat tidal zone. The recorded activities of ^{232}Th in the tidal flats were found significantly lower those downstream of the different valleys. The highest ^{232}Th was recorded at V. Araba (17.63Bq/kg), affected by the high activity recorded at the Gulf of Suez and Red sea during 2018. The valley downstream and the lowest activity (2.90Bq/kg) was recorded at Umm Hawytat tidal zone. V. Ambagy recorded the highest ^{40}K (345.78Bq/kg) and V. Abu Dabab recorded the lowest activity (44.80Bq/kg). In general, the significant decline in the natural radionuclides activities at the tidal flat zones except for ^{238}U at V. Hamrawin was attributed to many reasons; the biological activities at these zones, marine current effects that disperse the fine particles from the shallow zones and the effects of wave winnowing that remove particles.

Table 2. The mean activities of ^{238}U, ^{232}Th, and ^{40}K, and radiation hazard parameters along the Gulf of Suez and Red Sea during 2018.

Site	Zone	^{238}U	^{232}Th	^{40}K	D	AEDE	Ra_{eq}	H_{ex}	Iγr	ELCR
V. Al Galala	**Down stream**	29.36	27.36	336.44	44.12	54.11	94.39	0.25	0.69	154.42
V. Araba		24.23	29.92	426.45	47.05	57.70	99.85	0.27	0.75	164.67
V. Umm Hawytat		26.73	19.82	497.18	45.05	55.25	93.35	0.25	0.71	157.68
V. Hamrawin		93.20	27.98	394.58	76.41	93.71	163.59	0.44	1.16	267.44
V. Ambagy		20.30	17	296.23	32	39.24	67.42	0.18	0.50	112
V. Abu Dabab		22.43	14.53	328.01	32.82	40.24	68.46	0.18	0.51	114.85

Table 3. Comparison between the mean activities concentrations of ^{238}U, ^{232}Th and ^{40}K, and radiation hazard parameters along the Gulf of Suez and Red Sea.

Site	Zone	^{238}U	^{232}Th	^{40}K	D	AEDE	Ra_{eq}	H_{ex}	Iγr	ELCR
V. Al Galala	**Tidal Flat**	6.10	4.38	73.52	8.53	10.46	18.02	0.05	0.13	29.85
V. Araba		16.30	17.63	136.13	23.86	29.26	52.00	0.14	0.38	83.50
V. Umm Hawytat		4.40	2.90	87.20	7.42	9.10	15.26	0.04	0.12	25.97
V. Hamrawin		157.68	11.58	205.03	88.39	108.40	190.01	0.51	1.30	309.35
V. Ambagy		19.60	16.73	345.78	33.58	41.18	70.14	0.19	0.53	117.52
V. Abu Dabab		6.70	13.67	44.80	13.22	16.21	29.69	0.08	0.21	46.26

Table 4. Comparison between the main activity concentration of ^{238}U, ^{232}Th and ^{40}K of the present study with those of the other locations inside Egypt.

Location	^{238}U	^{232}Th	^{40}K	Reference
Red Sea valleys	6.10- 157.68	4.38-29.92	44.80-497.18	Present study
Hamrawin	-	8±0.1	282±7	**(Salah el Din & Vesterbacka, 2012)**
Safaga sand	-	21.4±10	618±122	**(El-Arabi, 2005)**
Hurghada sand	-	22.4±10	548±82	**(El-Arabi, 2005)**
Shore sediment	-	31.4±9.6	427.5±35	**(El-Mamoney & Khater, 2004)**
Suez canal	-	33-35.4	59-368	**(El-Tahawy *et al*., 1994)**
Qusier harbor	-	19(4-33)	458(16-2665)	**(El-Taher *et al*., 2018)**
Abutartour harbor	-	20(14-34)	430(378-511)	**(El-Taher *et al*., 2018)**
Touristic Harbor	-	21(15-32)	602(327-821)	**(El-Taher *et al*., 2018)**
Hurghada harbor	-	13(2-23)	489(36-950)	**(El-Taher *et al*., 2018)**
Zaranik North Sinai	-	214	77.7	**(Seddeek *et al*., 2005)**
El-Salam Canal	16.18	13.66	264.42	**(Ramadan *et al*., 2018)**

Red Sea	9.2	6.6	172.15	**(Salama *et al*., 2015)**
Burullus lake	17.22	10.03	299.7	**(Dar and El Saharty, 2012)**
Mariot lake	12.65	7.24	518.75	**(Dar and El Saharty, 2012)**
Ras El-Behar, R.S.	15.2	16.2	330.7	**(Dar and El Saman, 2012)**
Hamrawin, Red Sea	114.2	14.8	253.9	**(Dar and El Saman, 2012)**
Red Sea sediments	16.76	10.15	593.01	**(El Saharty and Dar, 2010)**
Burullus lake	14.3	20	312	**(El-Reefy *et al*., 2010)**
Idku lake	20.37	26.05	329.05	**(Fahmi *et al*., 2010)**
Safaga, Red Sea	25.3	21.4	618	**(El-Arabi, 2005)**
Hurghada, Red Sea	20.6	22.4	548	**(El-Arabi, 2005)**
Nasser lake	14.3-22	18.4-24.4	222-326	**(Khater *et al*., 2005)**

3. Radiation Hazard Indices:

3.1. Absorbed and Effective Dose Rate (D):

The D is the principal parameter to assess health risk, as biological, radiologic, and clinical impacts relay on the D. The highest value was found in the tidal flat zone of V. Hamrawin (88.39nGy h^{-1}), and the lowest values were found in tidal flat areas of V (Table 2). Umm Hawytat (7.42nGy h^{-1}) and V. Al Galala (8.53nGy h^{-1}). The D values of the different selected areas were found below the permissible level 55 $nGyh^{-1}$ **(UNSCEAR, 2000)**, except at the downstream and tidal flat areas of V. Hamrawin due to the high activities of phosphate ores grinding and shipment.

3.2. The Annual Effective Dose Effect (AEDE):

The results of AEDE rates for the different specimens are listed in (Table 2). V. Hamrawin downstream and tidal flat recorded the highest values of AEDE (93.71 and 108.40 $mSvy^{-1}$, respectively) compared to the different valleys, and the lowest value was found in the tidal flat of V. Umm Hawytat (9.10$mSvy^{-1}$). The AEDE values for the analyzed samples were found lower than the corresponding worldwide value of 73.67 $mSvy^{-1}$ **(UNSCEAR, 2000)** and does not represent any danger signs to humans except V. Hamrawin, which has AEDE value higher than the permissible level.

3.3. Radium Equivalent Activity Level Index (Ra_{eq}):

The major purpose of assessing natural radioactivity is to predict the possible radiation dose to be transmitted to living organisms. Various parameters can explain exposure to radiation; Ra_{eq} is a common hazard identification marker to explain the radiation exposure. Because of the non-uniform distributions of radionuclides in samples, Ra_{eq} has been defined as a single radiological parameter that compares the specific ^{238}U, ^{232}Th, and ^{40}K in the sediments **(Beretka & Mathew, 1985)**. **Table (2)** represented that V. Hamrawin downstream and tidal flat recorded the highest value of Ra_{eq} (163.59, 190.01Bq kg^{-1}, respectively) relative to the different valleys, and the lowest value was found in a tidal flat area of V. Al Galala (18.02Bq kg^{-1}). The Ra_{eq} values for the analyzed samples were found lower than the international recommended average of 370 Bq kg^{-1} **(UNSCEAR, 2000)** and the humans are not exposed to any radiological danger.

3.4. External Hazard Index (H_{ex}):

To assess the hazard of natural ɣ radiation, the H_{ex} was computed. The value of H_{ex} should be below one or negligible in order for the external hazard must be acceptable to the general public, and the radiation hazard must remain insignificant **(UNSCEAR, 1993; Varshney *et al*., 2010)**. In present study, the values of the H_{ex} in the examined samples were found less than unity at the downstream and tidal flat areas of the different valleys.

3.5. Representative Level Index (Iγr):

Table (2) represents the radioactivity level indices, where the lowest value 0.13 was found in the tidal flat zone of V. Al Galala, while the highest values were 1.30 and 1.16 found in tidal flat and downstream zones of V. Hamrawin respectively showed higher levels than the permissible level (≤1.00) according to **(UNSCEAR, 1993)**. The radioactivity level indices for studied valleys lie within the permissible limit except the tidal flat and downstream of V. Hamrawin.

Table 5. The radiological hazard parameters calculated in the sediment samples of the present study as compared with the previous studies inside Egypt.

Site	D (nGy h-1)	AEDE (µSv/y)	Ra_{eq} (Bq/kg)	H_{ex}	IƔr	ELCR	Reference
Red sea valleys	7.42-88.39	10.46-108.40	18.02-190.01	0.04-0.51	0.12-1.3	25.97-309.35	Present study
Timsah Lake	30.85	37.84	67.02	0.18	0.23	132.43	**(Dar *et al*., 2020)**
El-Salam Canal	27.14	33.28	56.06	0.15	0.42	-	**(Ramadan *et al*., 2018)**
Red Sea	15.7	19.25	32.2	0.07	0.24	67.38	**(Salama *et al*., 2015)**
Burullus Lake	26.62	32.65	59.17	0.15	0.42	114.26	**(Dar and El Saharty, 2012)**
Mariot Lake	32.01	39.26	70.19	0.17	0.5	137.4	**(Dar and El Saharty, 2012)**
Rasel Behar	30.69	37.65	63.81	0.17	0.48	131.776	**(Dar and El Saman, 2012)**
Hamrawin	72.35	88.73	154.88	0.42	1.08	310.56	**(Dar and El Saman, 2012)**
Red Sea sediment	38.78	47.56	76.94	0.21	0.61	166.46	**(El Saharty and Dar, 2010)**
Brullus Lake	31.79	38.99	66.92	0.181	0.5	136.455	**(El-Reefy *et al*., 2010)**
Idku Lake	36.06	44.22	73.94	0.2	0.56	154.784	**(Fahmi *et al*., 2010)**
Safaga, Red sea	50.38	61.79	103.49	0.28	0.8	216.27	**(El-Arabi, 2005)**
Hurghada, R.S.	45.9	56.29	94.828	0.26	0.73	197.01	**(El-Arabi, 2005)**
Nasser Lake	32.66	40.05	69.47	0.187	0.52	140.19	**(Khater *et al*., 2005)**
Suez Canal	26.45	32.44	56.66	0.153	0.42	113.534	**(El-Tahawy *et al*., 1994)**
World average	**60.07**	**73.67**	**129.69**	**0.35**	**0.95**	**257.84**	**(UNSCEAR, 2000)**

3.6. Excess Lifetime Cancer Risk (ELCR):

The values of ELCR in the studied valleys were ranged between $0.03\times10^{-3}$and 0.31×10^{-3}. All the samples show ELCR values lower than the world average (0.29×10^{-3}) **(Kapdan *et al*., 2011)** except the Tidal flat area of V. Hamrawin (0.31×10^{-3}).

Consequently, the cancer risk increment with increasing the exposure time for humans and/or in closed places as the Grinding factory at Hamrawin.

Finally, by comparing the results of calculated radiation hazards; D, AEDE, Ra_{eq}, H_{ex}, Iγr and ELCR obtained In the present study with the previous studies showed that, the values of radiation hazard indices were found close to the values of the previous studies that were recorded in some sites in Egypt, except for Hamrawin valley, which recorded the highest radiation hazards values **(Table 5)**.

4. Statistical Analysis:

As shown in **(Table 6)**, The obtained results of correlation coefficients indicated that the different radioactive nuclides; ^{238}U, ^{232}Th, and ^{40}K, were responsible for the recorded radiation parameters but with different intensities, the downstream zones of V. Al Galala, V. Araba, V. Umm Hawytat, V. Ambagy, and V. Abu Dabab, showed excellent positive correlations between the different radionuclides (^{238}U, ^{232}Th and ^{40}K) and radiation hazard indices (D, AEDE, Ra_{eq}, H_{ex}, Iγr and ELCR) indicated that the three radio-elements are responsible for the recorded hazards levels in the localities. In the tidal flat zone of W. Al Galala, ^{232}Th showed strong to excellent positive correlations with different indices, ^{40}K showed fair, positive correlations, meaning that ^{232}Th was the essential reason for the hazard parameters in the tidal zone of this valley. At the tidal flat of V. Araba, ^{238}U and ^{232}Th showed excellent positive correlations with the hazard parameters; a fair negative correlation with ^{40}K indicated that ^{238}U and ^{232}Th are the probable sources for the recorded hazard levels. At V. Umm Hawytat tidal flat, D, AEDE, and Iγr showed excellent negative correlations with the three radio-elements; inversely, Ra_{eq}, $H_{ex,}$ and ELCR showed excellent positive correlations with the three radio-elements. At V. Ambagy tidal flat, the three radioelements could be responsible for the recorded hazards levels, and at V. Abu Dabab tidal flat, ^{238}U was positive with D and AEDE, ^{232}Th showed positive with Ra_{eq} and H_{ex}. However, ^{40}K was found excellent positive with Iγr and ELCR. Therefore, all the recorded hazard parameters at these valleys were found within the permissibility limits determined by **(UNSCEAR, 1993; 2000)**.

^{238}U is the only responsible reason for the elevated radiation hazard in V. Hamrawin downstream and tidal flat, where ^{238}U showed excellent positive correlations with the different radiation hazard indices (D, AEDE, Ra_{eq}, H_{ex}, Iγr and ELCR) and a fair to strong correlation with ^{232}Th and ^{40}K, as shown in **(Fig. 3)**.

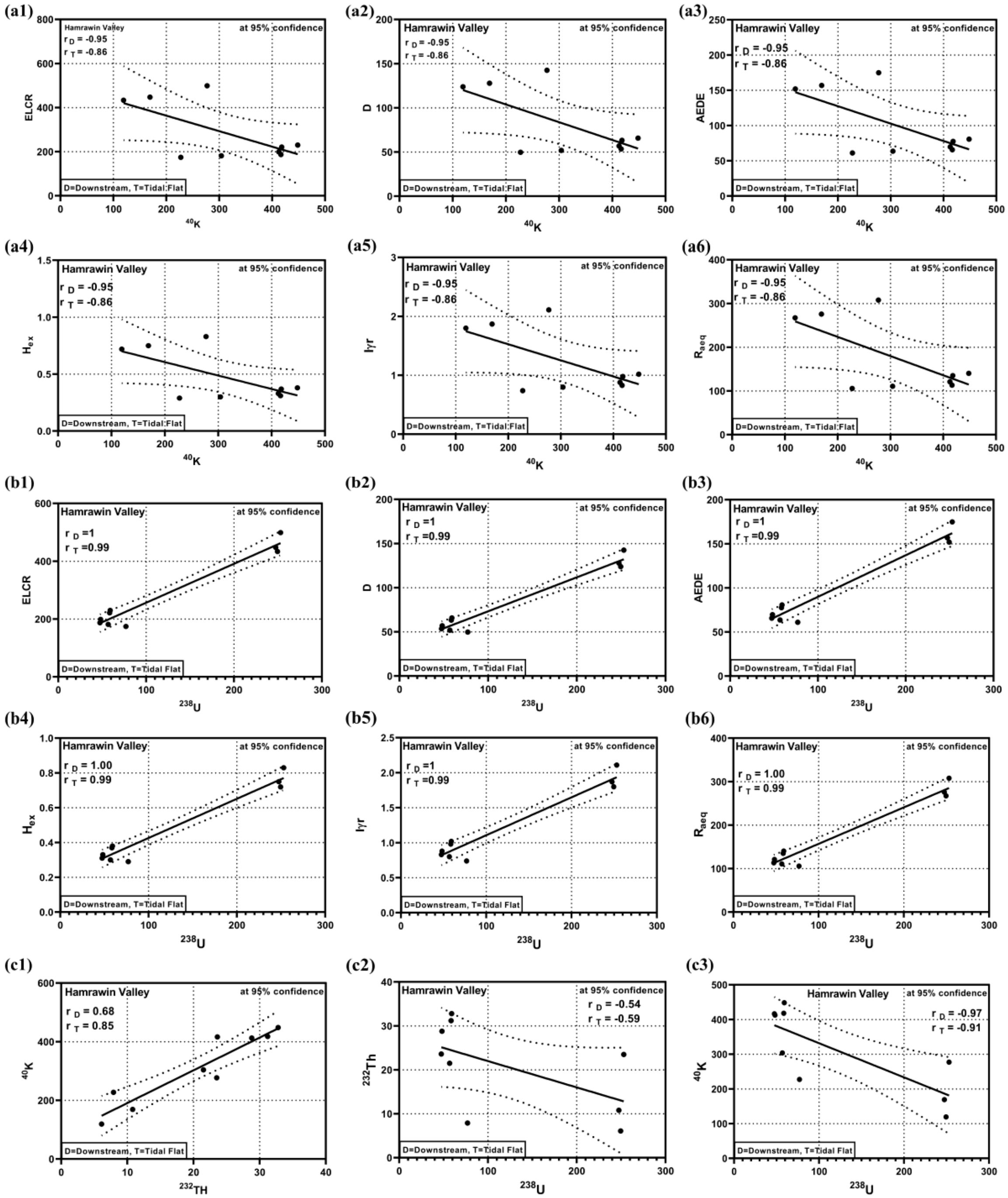

Fig. 3. Correlation Coefficients illustrate the relation between the radionuclides ^{238}U, ^{232}Th, ^{40}K, and radiation hazard parameters at Hamrawin valley.

Table 6. Correlation Coefficients illustrate the relation between the radionuclides ^{238}U, ^{232}Th, and ^{40}K, and radiation hazard parameters at the study valleys along the Gulf of Suez and the Red Sea during 2018.

Parameters		Downstream			Tidal flat		
		^{238}U	^{232}Th	^{40}K	^{238}U	^{232}Th	^{40}K
V.Al Galala	D	0.74	0.94	0.85	-0.26	0.83	0.58
	AEDE	0.74	0.94	0.85	-0.26	0.83	0.58
	Ra_{eq}	0.73	0.95	0.83	-0.14	0.89	0.47
	H_{ex}	0.73	0.95	0.83	-0.14	0.89	0.46
	Iγr	0.72	0.94	0.85	-0.28	0.82	0.60
	ELCR	0.74	0.94	0.85	-0.26	0.83	0.58
V.Araba	D	0.84	0.94	0.95	0.87	0.96	-0.64
	AEDE	0.84	0.94	0.95	0.87	0.96	-0.64
	Ra_{eq}	0.83	0.95	0.94	0.85	0.97	-0.67
	H_{ex}	0.83	0.95	0.94	0.85	0.97	-0.67
	Iγr	0.83	0.95	0.95	0.86	0.97	-0.66
	ELCR	0.84	0.94	0.95	0.87	0.96	-0.64
V.Umm Hawytat	D	0.72	0.85	0.86	-1.00	-1.00	-1.00
	AEDE	0.72	0.85	0.86	-1.00	-1.00	-1.00
	Ra_{eq}	0.72	0.87	0.84	1.00	1.00	1.00
	H_{ex}	0.72	0.87	0.84	1.00	1.00	1.00
	Iγr	0.70	0.87	0.87	-1.00	-1.00	-1.00
	ELCR	0.72	0.85	0.86	1.00	1.00	1.00
V.Hamrawin	D	1.00	-0.48	-0.95	0.99	-0.50	-0.86
	AEDE	1.00	-0.48	-0.95	0.99	-0.50	-0.86
	Ra_{eq}	1.00	-0.48	-0.95	0.99	-0.49	-0.86
	H_{ex}	1.00	-0.48	-0.95	0.99	-0.49	-0.86
	Iγr	1.00	-0.47	-0.95	0.99	-0.48	-0.86
	ELCR	1.00	-0.48	-0.95	0.99	-0.50	-0.86
V.Ambagy	D	0.99	1.00	0.97	0.76	0.88	0.78
	AEDE	0.99	1.00	0.97	0.76	0.88	0.78
	Ra_{eq}	0.99	1.00	0.97	0.78	0.90	0.74
	H_{ex}	0.99	1.00	0.97	0.78	0.90	0.74
	Iγr	0.99	1.00	0.97	0.74	0.88	0.79
	ELCR	0.99	1.00	0.97	0.76	0.88	0.78
V.Abu Dabab	D	0.63	0.85	0.94	1.00	-1.00	1.00
	AEDE	0.84	0.85	0.94	1.00	-1.00	1.00
	Ra_{eq}	0.84	0.85	0.94	-1.00	1.00	-1.00
	H_{ex}	0.84	0.85	0.94	-1.00	1.00	-1.00
	Iγr	0.82	0.86	0.95	1.00	-1.00	1.00
	ELCR	0.84	0.81	0.94	-1.00	-1.00	1.00

CONCLUSION

The natural radioactivity of the sediment samples in the valleys along the Gulf of Suez and the Red Sea was determined. The measured activity levels of the examined radioisotopes (^{238}U, ^{232}Th, and ^{40}K) in the studied valleys were found very changeable and rely on their radioactive mineral content. The average activity levels for ^{238}U, ^{232}Th, and ^{40}K in all selected zones were found lower than the worldwide reference levels except for Hamrawin valley, which is slightly higher than the worldwide average for ^{238}U activity, and Valleys of Araba and Umm Hawytat, which are slightly higher than the recommended worldwide average for ^{232}Th activity. The radiological risk parameters: D, AEDE, Ra_{eq}, H_{ex}, Iγr and ELCR values indicated that all the sites are safe and have no health risk for the population except Hamrawin valley, which had (D), (AEDE), (Iγr) and (ELCR) values higher than the Permissible levels.

REFERENCES

Abbasi, A.; Zakaly, H.M.H.; Algethami, M. and Abdel-Hafez, S.H. (2022). Radiological risk assessment of natural radionuclides in the marine ecosystem of the northwest Mediterranean Sea. Int. J. Radiat. Biol., 98: 205-211. https://doi.org/10.1080/09553002.2022.2020359

Al-Trabulsy, H.A.; Khater, A.E.M. and Habbani, F.I. (2011). Radioactivity levels and radiological hazard indices at the Saudi coastline of the Gulf of Aqaba. Radiat. Phys. Chem., 80(3): 343-348. https://doi.org/10.1016/j.radphyschem.2010.09.002

ASTM American Society for Testing Materials (1983). Standard Method for sampling surface soils for radionuclides. Philadelphia, PA, Report: C, pp. 983-998.

ASTM American Society for Testing Materials (1986). Recommended practice for investigation and sampling soil and rock for engineering purposes. In: “Annual Book of ASTM Standards (04.08)”, Philadelphia, PA, Report: D. 420, pp. 109-113.

ATSDR Agency for Toxic Substances and Disease Registry (1988). U.S. Department of Health and Human Services. Biennial Report, Volume II, Report for October 1986-December 1988.

Awad, H.A.; Zakaly, H.M.H.; Nastavkin, A.V.; El Tohamy, A.M. and El-Taher, A. (2021). Radioactive mineralizations on granitic rocks and silica veins on shear zone of El-Missikat area, Central Eastern Desert, Egypt. Appl. Radiat. Isot., 168(109493): 1-8. https://doi.org/10.1016/j.apradiso.2020.109493

Bell, F.G.; Lindsay, P. and Hytiris, N. (1997). Contaminated ground and contaminated estuary sediment illustrated by two case histories. Environ. Geol., 32(3): 191-202. https://doi.org/10.1007/s002540050207

Beretka, J. and Mathew, P.J. (1985). Natural radioactivity of Australian building materials, industrial wastes and by-products. Health Phys., 48: 87-95. https://doi.org/10.1097/00004032-198501000-00007

Boggs, S. (2009). Petrology of sedimentary rocks, second ed. Cambridge Univ. Press, Cambridge, England, ISBN: 9780511626487. https://doi.org/10.1017/ CBO 9780511626487

Dar, M.A. (2005). Coastal habitats degradation due to chronic and recent landfilling along the Red Sea. In: "First Ain Shams Univ. Int. Conf. on Environ. Eng.", Cairo, Egypt, 9-11 April, pp. 773-786.

Dar, M.A. and El Saharty, A.A. (2013). Activity levels of some radionuclides in mariout and brullus lakes, Egypt. Radiat Prot Dosimetry 157:85-94. https://doi.org/10.1093/rpd/nct106

Dar, M.A. and El Saman, M.I. (2012). The radiation hazards of some radio-elements in petroleum and phosphate regions along the Red Sea, Egypt. Third Int. Conf. on Radiat. Sci. and Appl., Hurghada, Egypt, 12-16 November, 5(2): 650-673. Accessed 23 May 2022, https://inis.iaea.org/collection/NCLCollection Store/_Public/44/104/44104865.pdf

Dar, M.A.; Uosif, M.A.; Mohamadeen, L.I.; El Saharty, A.A.; Zakaly, H.M. and Murad, F.A. (2015). The semi-annual variations of the bio-available heavy metals and natural radionuclides in Timsah Lake sediments, Egypt. Int. J. Sci. Eng. Res., 6(5): 1697-1712. Accessed 20 Mar 2022, https://www.ijser.org/research-paper-publishing-may-2015_page9.aspx

Dar, M.A.; Uosif, M.A.; Mohamadeen, L.I.; Madkour, A.G. and Zakaly, H.M. (2020). Radiation Hazards and the Cancer Risk Assessments in the Sediments of Timsah Lake, Egypt. J. King Abdulaziz Univ. Mar. Sci., 30(1): 1-16. https://doi.org/10.4197/mar.30-1.1

El-Arabi, A.M. (2005). Natural radioactivity in sand used in thermal therapy at the Red Sea Coast. J. Environ. Radioact., 81: 11-19. https://doi.org/10.1016/j.jenvrad.2004.11.002

El-Gamal, H.; Sidique, E. and El-Azab Farid, M. (2018). Considerable radioactivity levels in the granitic rocks of the central areas of the Eastern Desert, Egypt. Environ. Sci. Pollut. Res., 25: 29541-29555. https://doi.org/10.1007/s11356-018-2998-7

El-Mamoney, M. and Rifaat, A. (2001). Discrimination of Sources of Barium in Beach Sediments, Marsa Alam-Shuqeir, Red Sea Coast, Egypt. J. King Abdulaziz Univ. Mar. Sci., 12: 149-160. https://doi.org/10.4197/mar.12-1.11

El-Reefy, H.I.; Sharshar, T.; Elnimr, T. and Badran, H. (2010). Distribution of gamma-ray emitting radionuclides in the marine environment of the Burullus Lake: II. Bottom sediments. Environ. Monit. Assess., 169: 273-284. https://doi.org/10.1007/s10661-009-1169-1

El-Tahawy, M.S.; Farouk, M.A.; Ibrahiem, N.M. and El-Mongey, S.A.M. (1994). Natural and artificial radionuclides in the Suez Canal bottom sediments and stream water. Radiat. Phys. Chem., 44: 87-89. https://doi.org/10.1016/0969-806X(94)90110-4

El-Taher, A.; Alshahri, F. and Elsaman, R. (2018a). Environmental impacts of heavy metals, rare earth elements and natural radionuclides in marine sediment from Ras Tanura, Saudi Arabia along the Arabian Gulf. Appl. Radiat. Isot., 132: 95-104. https://doi.org/10.1016/j.apradiso.2017.11.022

El-Taher, A.; Zakaly, H.M.H. and Elsaman R. (2018b). Environmental implications and spatial distribution of natural radionuclides and heavy metals in sediments from four harbours in the Egyptian Red Sea coast. Appl. Radiat. Isot., 131: 13-22. https://doi.org/10.1016/j.apradiso.2017.09.024

El Mamoney, M.H. and Khater, A.E.M. (2004). Environmental characterization and radio-ecological impacts of non-nuclear industries on the Red Sea coast. J. Environ. Radioact., 73(2): 151-168. https://doi.org/10.1016/j.jenvrad.2003.08.008

El Saharty, A.A. and Dar, M.A. (2010). The concentration levels of some isotopic radionuclides in the coastal sediments of the Red Sea, Egypt. Isot. Radiat. Res., 42(1): 11-27. Accessed 15 March 2022, http://www.merrcac.com/mag42p1/mag2.pdf

El Samad, O.; Baydoun, R.; Nsouli, B. and Darwish, T. (2013). Determination of natural and artificial radioactivity in soil at North Lebanon province. J. Environ. Radioact., 125:36-39. https://doi.org/10.1016/j.jenvrad.2013.02.010

El Zrelli, R.; Rabaoui, L.; Abda, H.; Daghbouj, N.; Pérez-López, R.; Castet, S.; Aigouy, T.; Bejaoui, N. and Courjault-Radé, P. (2019). Characterization of the role of phosphogypsum foam in the transport of metals and radionuclides in the Southern Mediterranean Sea. J. Hazard. Mater., 363: 258-267. https://doi.org/10.1016/j.jhazmat.2018.09.083

Fahmi, N.M.; El-Khatib, A.; Abd El-Salam, Y.M.; Shalaby, M.H.; El-Gally, M.M. and Naim, M.A. (2010). Study of the environmental impacts of the natural radioactivity presents in beach sand and Lake Sediment samples Idku, Behara, Egypt. In: Proceedings of the 10th Radiation Physics & Protection Conference, Nasr City - Cairo, Egypt, 27-30 November, pp. 391-402. Accessed 16 March 2021, https://inis.iaea.org/collection/NCLCollectionStore/_Public/42/076/42076665.pdf

INRS (Institut National de Recherche et de Sécurité) (2012). Limit values for occupational exposure to chemical agents in France, Diquat Edition: Technical Memory Help (In French: Valeurs limites d'exposition professionnelle aux agents chimiques en France. Édition Diquat 984: Aide-Memoire Technique, Institut. Nation. In: ED 984: 1-9. Accessed 12 March 2022, https://www.inrs.fr/publications/bdd/fichetox/fiche.html?refINRS=FICHETOX_288

Jacobi, W. (1988). Assessment of Dose from man-made Sources. In: Radionuclides in the Food Chain. Springer, London, pp. 45-57. https://doi.org/10.1007/978-1-4471-1610-3_5

Janković, M.; Todorović, D.; Savanović, M. (2008). Radioactivity measurements in soil samples collected in the Republic of Srpska. Radiat. Meas., 43: 1448-1452. https://doi.org/10.1016/j.radmeas.2008.03.004

Kapdan E.; Varinlioglu, A. and Karahan, G. (2011). Radioactivity Levels and Health Risks due to Radionuclides in the Soil of Yalova, Northwestern Turkey. Int. J. Environ. Res., 5:837-846. https://doi.org/10.22059/ijer.2011.441

Khater, A.E.; Ebaid, Y.Y. and El-Mongy, S.A. (2005). Distribution pattern of natural radionuclides in Lake Nasser bottom sediments. Int. Congr. Ser., 1276: 405-406. https://doi.org/10.1016/j.ics.2004.11.112

Mahur, A.K.; Kumar, R.; Mishra, M.; Ali, S.A.; Sonkawade, R.G.; Singh, B.P.; Bhardwaj, V.N. and Prasad, R. (2010). Study of radon exhalation rate and natural radioactivity in soil samples collected from East Singhbhum Shear Zone in Jaduguda U-Mines Area, Jharkhand, India and its radiological implications. Indian J. Pure. Appl. Phys., 48(7):486-492. Accessed 26 March 2022, http://nopr.niscair.res.in/handle/123456789/9905

Nasr, S.; El-gamal, A.; Hendawi, I. and Naim, M. (2006). Statistical Evaluation of Natural Radioactivity in Sediments Along the Egyptian Mediterranean Coast. The 2nd Environ. Phys. Conference (EPC 06), Alexandria, Egypt, 18-22 Feb.

Noureddine, A.; Baggoura, B.; Hocini, N. and Boulahdid, M. (1998). Uptake of radioactivity by marine surface sediments collected in Ghazaouet, West coast of Algeria. Appl. Radiat. Isot., 49(12):1745-1748. https://doi.org/10.1016/S0969-8043(97)10117-8

Ramadan, A.; Abu-Zeid, H.M.; Talaat, S.M.; Abd El-Maksoud, T.M.; Sayed, H. and El-Hanbaly, A.H. (2018). Evaluation of Natural Radioactivity and Physico-Chemical Characteristics along El-Salam Canal, Egypt. Int. J. Eng. Sci. Invent., 7(4- IV):51-63. Accessed 23 May 2022, http://ijesi.org/papers/Vol(7)i4/Version-4/H0704045163.pdf

Ramasamy, V.; Sundarrajan, M.; Paramasivam, K.; Meenakshisundaram, V. and Suresh, G. (2013). Assessment of spatial distribution and radiological hazardous nature of radionuclides in high background radiation area, Kerala, India. Appl. Radiat. Isot. 73:21-31. https://doi.org/10.1016/j.apradiso.2012.11.014

Ravichandran, G.; Rathnakar, G.; Santhosh, N. and Thejaraju, R. (2019). Antiwear performance evaluation of halloysite nanotube (HNT) filled polymer nanocomposites. Int. J. Eng. Adv. Technol., 9:3314-3321. https://doi.org/10.35940/ijeat.A1469.109119

Salah el Din, K. and Vesterbacka, P. (2012). Radioactivity levels in some sediment samples from Red sea and Baltic Sea. Radiat. Prot. Dosim., 148(1): 101-106. https://doi.org/10.1093/rpd/ncq591

Salama, E.; Diab, H.M.; EL-Fiki, S.A. and Ibrahim, A. (2015). Distribution of Radionuclides in Soil and Beach Samples of the Western Coast of Suez Gulf, Egypt. Arab J. Nucl. Sci. Appl., 48(2): 63-69. Accessed 15 March 2002, http://www.esnsa-eg.com/DetailsJournal.aspx?ID=14

Seddeek, M.K.; Badran, H.M.; Sharshar, T. and Elnimr, T. (2005). Characteristics, spatial distribution and vertical profile of gamma-ray emitting radionuclides in the coastal environment of North Sinai. J. Environ. Radioact., 84(1):21-50. https://doi.org/10.1016/j.jenvrad.2005.03.005

Shetty, P.K. and Narayana, Y. (2010). Variation of radiation level and radionuclide enrichment in high background area. J. Environ. Radioact., 101:1043-1047. https://doi.org/10.1016/j.jenvrad.2010.08.003

Taskin, H.; Karavus, M.; Ay, P.; Topuzoglu, A.; Hidiroglu, S. and Karahan, G. (2009). Radionuclide concentrations in soil and lifetime cancer risk due to gamma radioactivity in Kirklareli, Turkey. J. Environ. Radioact., 100:49-53. https://doi.org/10.1016/j.jenvrad.2008.10.012

UNSCEAR United Nations Scientific Committee on the Effects of Atomic Radiation (1993). Sources and Effects of Ionizing Radiation, Report to the General Assembly, with scientific annexes, Annex C. United Nations Publication, New York, USA, ISBN: 92-1-142200-0, pp. 280-283. Accessed 15 March 2022, https://www.unscear.org/unscear/en/publications/scientific-reports.html

UNSCEAR United Nations Scientific Committee on the Effects of Atomic Radiation (2000). Sources and Effects of Ionizing Radiation, Report to the General Assembly, with scientific annexes, Vol. I: Sources, Annex B: Exposures from natural radiation sources. United Nations Publication, New York, USA, ISBN: 92-1-142238-8, Accessed 16 March 2022, https://www.unscear.org/unscear/en/publications/scientific-reports.html

UNSCEAR United Nations Scientific Committee on the Effects of Atomic Radiation (2008). Sources and Effects of Ionizing Radiation. Report to the General Assembly with scientific annexes, Vol. I, Annex B: Exposures of the public and workers from various sources of radiation. United Nations Publication, New York, USA, ISBN: 978-92-1-142274-0, Accessed 16 March 2022, https://www.unscear.org/unscear/en/publications/2008_1.html

Varshney, R.; Mahur, A.K.; Sonkawade, R.G.; Suhail, M.A.; Azam, A. and Prasad, R. (2010). Evaluation and analysis of ^{226}Ra, ^{232}Th, ^{40}K and radon exhalation rate in various grey cements. Indian J. Pure. Appl. Phys., 48:473-477. Accessed 16 March 2022, http://nopr.niscair.res.in/handle/123456789/9902

Yücel, H.; Övüç, S.; Akkaya, G. and Çakmak, Ş. (2020). Estimation of radiological exposure levels in a mining area based on ^{238}U, ^{226}Ra, ^{232}Th and ^{40}K activity measurements: A case study for Beylikova-Sivrihisar Complex Ore site in Turkey. Radiat. Prot. Dosim., 190(3):297-306. https://doi.org/10.1093/rpd/ncaa104

Zakaly, H.M.; Uosif, M.A.; Madkour H.; Tammam, M.; Issa, S.; Elsamman, R. and El-Taher, A. (2019). Assessment of Natural Radionuclides and Heavy Metal Concentrations in Marine Sediments in View of Tourism Activities in Hurghada City, Northern Red Sea, Egypt. J. Phys. Sci., 30(3):21-47. https://doi.org/10.21315/jps2019.30.3.3

Zakaly, H.M.H.; Uosif, M.A.M.; Issa, S.A.M.; Tekin, H.O.; Madkour, H.; Tammam, M.; El-Taher, A.; Alharshan, G.A. and Mostafa, M.Y.A. (2021). An extended assessment of natural radioactivity in the sediments of the mid-region of the Egyptian Red Sea coast. Mar. Pollut. Bull., 171:112658. https://doi.org/ 10.1016/J.MARPOLBUL.2021.112658